miR-29c promotes alcohol dehydrogenase gene cluster expression by activating the enhancer within ADH6

Ningning Chen
Qingdao University
Jiao Luo
Qingdao University
Yufei Hou
Weihai Center for Disease Control and Prevention
Yanan Ji
Qingdao University
Mengyue Xie
Qingdao University
Ge Song
Qingdao University
Dianke Yu (dianke.yu@qdu.edu.cn)
Qingdao University

Research Article

Keywords: Ethanol, miR-29c, Alcohol Dehydrogenase Gene Cluster, ADH6, Enhancer

Posted Date: April 20th, 2022

DOI: https://doi.org/10.21203/rs.3.rs-1563020/v1

Abstract

Alcohol dehydrogenases (ADHs) play vital roles in alcohol metabolism and alcohol toxicity, yet little is known about miRNA-mediated regulation of *ADH* gene cluster. Here, we showed that miR-29c might activate *ADH* gene cluster transcription by targeting an enhancer element within *ADH6* gene. miR-29c is differentially expressed in alcoholic liver disease. Following biochemical and molecular evidences demonstrated that miR-29c could increase *ADH6* mRNA and protein levels without affecting the stability of *ADH6* transcript. Further evidence showed that exogenous miR-29c could move into the nucleus and then unconventionally bound an enhancer element within *ADH6* gene. Luciferase reporter assay and chromatin immunoprecipitation data indicated that miR-29c could activate the enhancer and increase the enrichment of RNA Polymerase II at the promoter region of *ADH1A*, *ADH1B*, *ADH1C*, *ADH4*, and *ADH6*. Finally, exogenous miR-29c transfection promoted the expressions of *ADH1A*, *ADH1B*, *ADH1C*, and *ADH4* pre-mRNA and mRNA transcripts in the *ADH* gene cluster. In conclusion, our data suggest that miR-29c might represent as a novel epigenetic regulator involved in ADH gene cluster activation.

1 Introduction

Chronic and excessive alcohol drinking induces a wide spectrum of hepatic lesions, the most typical of which include steatosis, hepatitis, and fibrosis/cirrhosis (Bajaj, 2019). Alcohol-associated liver disease (ALD) accounts for approximately 3 million deaths *per* year, and is a major driver of global liver-related morbidity and mortality (Han et al., 2021; Rehm, Samokhvalov, & Shield, 2013). A great deal of research has proved that the principal cause of alcoholic liver injury depends on the concentrations of ethanol and its metabolites in the body (Haseba & Ohno, 2010). For example, excessive ethanol oxidation resulted in the production of large amounts of reactive oxygen species, which further attack hepatocytes, Kupffer cells, stellate cells, and liver sinusoidal endothelial cells, initiating liver injury including steatosis, fibrosis, and cirrhosis in susceptible individuals with specific risk factors (B. Gao, Ahmad, Nagy, & Tsukamoto, 2019; Saikia et al., 2017; Teschke, 2018). Worse yet, acetaldehyde, an oxidation product of alcohol, has capable of initiating carcinogenesis by forming adducts with proteins and DNA and causing mutations (Bhatia, Drake, Miller, & Wells, 2019; Marshall et al., 2018; Rumgay, Murphy, Ferrari, & Soerjomataram, 2021).

Alcohol dehydrogenase (ADH), along with aldehyde dehydrogenase (ALDH), was well known as the primary enzymes responsible for alcohol metabolism *in vivo*, and the former metabolized ethanol to acetaldehyde, and the latter then metabolized the resulting acetaldehyde to acetic acid (Teschke, 2018). The human ADH genes, including *ADH1A*, *ADH1B*, *ADH1C*, *ADH4*, *ADH5*, *ADH6*, and *ADH7*, are distributed in a gene cluster on chromosome 4. Currently, considerable efforts have been made about the effects of ADH expression or activity imbalance on health effects (N. Gao et al., 2018; Jelski et al., 2017; Jelski & Szmitkowski, 2008), but the contributors of the ADH expression change have still not been clarified.

MicroRNA (miRNA), a class of 22 nt non-coding RNA, typically functions as epigenetic modulators to regulate gene expression at the post-transcriptional levels. Yet some reports also showed that some

miRNAs are present in the nucleus and exert their functions by targeting genomic DNA sequence (Majid et al., 2010; Santovito et al., 2020; Xiao et al., 2017). Many miRNAs, *e.g.* miR-122 (Satishchandran et al., 2018), miR-155 (Bala et al., 2016), and miR-34a (Iwagami et al., 2018), have been shown to regulate inflammation, lipid accumulation, and fibrosis in ALD. However, few studies focused on the regulatory roles of miRNAs in alcohol metabolism. Our recent study has elucidated a positive regulatory role of has-miR-148a on ADH4 in ethanol exposed hepatic cells (Luo et al., 2021). Furthermore, a few miRNAs have been reported to target enhancer sequences and promote the expression of neighboring genes (Xiao et al., 2017). As ADH genes are present in a gene cluster, this drives us to explore whether miRNAs function as positive regulators in ADH gene cluster expression.

miR-29c, a tumor suppressor, has been shown to be silenced or down-regulated in many different types of cancer (Schmitt, Margue, Behrmann, & Kreis, 2013). Recently, increasing evidences have indicated that miR-29c was highly correlated with the disease severity of ALD (Liu, Chen, Jin, & Li, 2013; Yao et al., 2019), nevertheless, its mechanism of function is rarely understood. In this study, using correlation analysis and *in silico* prediction, we predicted *ADH6* as a target gene of miR-29c and elucidated an unconventional regulatory mechanism of miR-29c on ADH gene cluster expressions by activating enhancer. Thus, we anticipate that the transcriptional activation of the *ADH* gene cluster by miR-29c may be a novel pathway contributing to ALD.

2 Methods

2.1 Cell culture and treatment

The hepatocellular carcinoma Huh7 cell line was obtained from the Cell Bank of Chinese Academy of Sciences (Shanghai, China) and HEK-293 FT cells were obtained from American Tissue Type Culture Collection (ATCC, Manassas, VA, USA). Both cell lines were cultured in DMEM medium that supplemented with 10% fetal bovine serum (FBS). ADH1 overexpressed Huh7 cell ($Huh7^{ADH1}$) was established as described previously (Luo et al., 2021). Briefly, a revised plenty-CMV-IRES Puromycin lentivirus expression vector was constructed using an In-fusion cloning method. Then Huh7 cells were infected with lentivirus, which was collected after 48 h transfection. Finally, $Huh7^{ADH1}$ cells were obtained after puromycin treatment.

miR-29c mimics and control mimics were synthesized by GE Dharmacon (Denver, CO, USA). Huh7 and $Huh7^{ADH1}$ cells were transfected with the mimics or control using Lipofectamine RNAiMAX reagents (Invitrogen, Carlsbad, CA, USA), according to the manufacturer's instructions. Cells were exposed to 0, 50, 100, 200, and 400 mM ethanol (Sinopharm, Beijing, China), cultured in a 37°C incubator containing 5% $CO_{2,}$ and saturated with 200 mM alcohol to slow down the evaporation of ethanol in the medium (Thompson et al., 2016; You, Fischer, Deeg, & Crabb, 2002).

2.2 RNA extraction, reverse transcription, and quantitative real-time PCR (qRT-PCR)

Total RNA from cells was extracted using Trizol reagent (Invitrogen), and the RNA from the cytoplasm and nucleus was separated by a Nuclear and Cytoplasmic Extraction Reagents Kit (Thermo Scientific, Waltham, MA, USA), according to the manufacturer's instructions. The reverse transcription and quantification of genes and miRNA were performed, as the previously described method (Luo et al., 2021). The miRNA levels were normalized to U6 snRNA, while the relative mRNA levels were normalized to *ACTB*. The sequences of the primers used in this study are shown in Supplementary Table 1, and all experiments were performed at least three times.

2.3 Western blot analysis

Protein samples were extracted from cells by using RIPA buffer (Thermo Scientific) supplemented with the protease inhibitor cocktail (MedChemExpress, NJ, USA). Total protein concentrations were quantitated via the BCA method (Thermo Scientific), and then equal amounts of proteins samples were subjected to SDS-PAGE, followed by immunoblotting. Primary antibodies anti-ADH1A (ab108203), anti-ADH1B (ab175515), anti-ADH1C (ab168748), anti-ADH4 (ab137077), anti-ADH5 (ab177932), anti-AGO1 (ab5070), anti-AGO2 (ab156870) were purchased from Abcam (Cambridge, MA, USA). Anti-ADH6 was purchased from Santa Cruz (CA, USA), and anti-β-Actin (AC-15, Boster, Wuhan, China) was used as a control antibody. After HRP-conjugated secondary antibody incubation, the target band was detected using the chemiluminescence system (Tanon 5200, Shanghai.China).

2.4 Cellular localization of synthetic Cy3-labeled miR-29c

For the localization analysis of miR-29c, the Cy3-labeled miR-29c mimics and negative control Cy3-labeled miR-29a were transiently transfected into Huh7 cells. After 48h incubation, cells were washed by PBS three times and fixed with 4% paraformaldehyde for 30 min at 37°C. Then, the cells were washed and stained with DAPI. Fluoresce signaling was detected and imaged with Olympus fluorescence microscope (Japan).

2.5 Luciferase reporter gene assay

To determine the regulation effect of miR-29c on target enhancer activity, the enhancer region of *ADH6* that contains the response elements of miR-29c and mutation site were subcloned into the PGL3-promoter vector, respectively. Next, the resultant constructs were transfected into HEK-293 FT cells together with the chemically synthetic miR-29c mimics or control mimics, respectively, in a white 96-well clear-bottom plate. After 48 h incubation, the *Firefly* luciferase activities were measured using the Dual-Glo Luciferase Assay System (Promega, Madison, WI, USA). pRL-SV40 plasmid expressing *Renilla* luciferase was used to normalize the *Firefly* luciferase activity.

2.6 Fluorescent-based RNA electrophoretic mobility shift assay (FREMSA)

The miR-29c oligonucleotide labeled with IRDye™ 800 was designated as Dye-miR-29c, while the DNA oligonucleotides, i.e., the miR-29c response element resident in the DNA sequence of *ADH6*, were 5'-modified with Cy5.5™ and designated as Short Dye gene and Long Dye gene, respectively. FREMSA

assays were carried out as described in the previous study with minor modifications (Chen et al., 2015). Briefly, Dye-labeled oligonucleotides were first heated at 95°C for 2 min and subsequently cooled down on the ice. Then the Short Dye gene or Long Dye gene oligonucleotides (final concentration: 400 nM) with Huh7 nuclear extracts were added to the reaction systems according to the instructions of LightShift Chemiluminescent RNA EMSA Kit (Thermo Scientific), respectively, and incubated for 20 min at room temperature. The reaction mixtures were then separated by 6% native PAGE electrophoresis at 4°C, and visualized by the Odyssey CLx Infrared Imaging System from LI-COR Biosciences (Lincoln, NE, USA).

2.7 RNA immunoprecipitation (RIP)

RIP assay was conducted using the Imprint® RNA Immunoprecipitation Kit (Sigma-aldrich, St. Louis, MO, USA), according to the manufacturer's protocols. Huh7 cells were first lysed with Mild Lysis Buffer containing EDTA-free protease inhibitor cocktail and then centrifuged for 10 min at 16,000×g at 4°C. Antibodies against AGO1 and AGO2 were mixed with magnetic beads coated with protein A/G and incubated with constant rotation for 30 min at room temperature, respectively. Subsequently, the anti-AGO1 and anti-AGO2 antibody and protein A/G-coated magnetic beads were mixed with the lysates and incubated at 4°C overnight. After precipitation and washing, the immunoprecipitated RNA samples were then extracted and reverse transcribed with specific primers, followed by qRT-PCR. Finally, the results were normalized to input RNA levels.

2.8 miRNA pulldown assay

miRNA pulldown assay was conducted according to the method previously described (Luo et al., 2021). miR-29c mimics and miR-NC mimics with 3'-modified by the biotin were first synthesized in RiboBio (Guangzhou, China), and then transfected into Huh7 cells at the final concentration of 20 nM, respectively. After incubation overnight, the cells were then lysed using the lysis buffer and then incubated with the Dynabeads MyOne Streptavidin C1 beads (Thermo scientific) for 4 h at 4°C to capture the complex containing biotin–miRNA and the cognate mRNA. Eventually, the pulldown lysates were used for RNA extraction and analyzed by qRT-PCR. The products of PCR were analyzed by agarose gel electrophoresis.

2.9 mRNA degradation assay

After transfection of the miR-29c -3p mimics or control mimics for 24h, Huh7 cells were treated with actinomycin D, at the final concentration of 5 μg/ml. The cells were harvested at 0, 2, 4, 8, 16, and 24 h after actinomycin D treatment, respectively, and total RNAs were prepared to test the relative *ADH6* transcript levels as mentioned above. *GAPDH* was used for normalization.

2.10 Chromatin immunoprecipitation (ChIP)

Ten million cells and 5 μg antibodies were used for each ChIP assay. The following antibodies were used for ChIP: H3K4me3 (ab8580), H3K27ac (ab4729), H3K4me1 (ab8895), rabbit IgG (ab171870), and RNA polymerase II antibody (ab264350), and experiments were carried out according to the manufacturer's

instructions for Pierce Magnetic ChIP Kit (Thermo Scientific). After eluting with 1 × IP Elution Buffer, the purified DNA was detected by quantitative PCR with specific primers.

2.11 Transposase-Accessible Chromatin Sequencing (ATAC-seq)

Genome-wide measurement of chromatin accessibility of the cell was performed using ATAC-Seq. Briefly, the nuclei from miR-29c mimics and control mimics treated Huh7 cells were lysed and spun at 500×g for 5 min to remove the supernatant. The nuclei pellet was then incubated with the Tn5 transposase, which inserts sequencing adapters into accessible regions of chromatin. Adapter-ligated DNA fragments are then isolated, amplified by PCR, and used for next-generation sequencing. After data filtering, the clean data were mapped to the reference genome (hg38) using Bowtie2 (Version: 2.2.5). MACS software S (Model-based Analysis for ChIP-Seq, version: 2.1.0) was applied to locate the enriched regions of reads on the genome.

To identify differential peaks between samples, we first assumed that the true intensities of most common peaks are the same between two ATAC-Seq samples. Second, the observed differences in sequence read density in common peaks is presumed to reflect the scaling relationship of ATAC-Seq signals between two samples, which can thus be applied to all peaks. Based on these hypotheses, the $\log_2$ ratio of read density between two samples M was plotted against the average $\log_2$ read density A for all peaks, and robust linear regression was applied to fit the global dependence between the M-A values of common peaks. Then the derived linear model was used as a reference for normalization and extrapolated to all peaks. Finally, the *P*-value for each Peak was calculated based on Bayesian model, the significant regions were picked up if $|M| \geq 1$ and *P*-value $\leq 10^{-5}$.

2.12 Statistical analyses

The results obtained in this study were depicted as the mean ± standard deviation (SD) and analyzed with Student's *t*-tests or one-way ANOVA using GraphPad Prism version 7.0 (GraphPad). $P < 0.05$ was considered statistically significant. The correlation coefficients (*r*) were calculated by Pearson correlation analysis, and the absolute value of $r > 0.2$ was considered to be correlated.

3 Results

3.1 Decreased miR-29c and ADH6 expression *in vivo* and *in vitro* upon ethanol exposure

To explore the potential relationship between ADH cluster and miR-29c, we first analyzed the expression correlations between miR-29c and *ADH* cluster genes, including *ADH1A*, *ADH1B*, *ADH1C*, *ADH4*, *ADH5*, *ADH6* and *ADH7*. Results showed that miR-29c exhibited positive correlations with *ADH1A*, *ADH1B*, *ADH1C*, *ADH4* and *ADH6* mRNA levels in normal human livers, but no correlations with *ADH5* and *ADH7* expression (Fig. 1a). Next, we analyzed whether there are potential binding sites for miRNA in *ADH* cluster

genes using RNAhybrid tools (bibiserv.cebitec.unibielefeld.de-/rnahybrid/). As a result, we uncovered that only the *ADH6* was the putative target of the miR-29c (Fig. 1b). Thus, ADH6 was selected as potential targets for further analysis. We then analyzed the expression status of the miR-29c and *ADH6* by *in vitro* and *in vivo* models. As shown in Fig. 1c, endogenous miR-29c and *ADH6* RNA levels in the liver samples of AH patients obtained from the GSE28619 dataset were significantly lower than those in normal individuals, respectively (36.98% and 17.16%, respectively; all $P < 0.05$). In *in vitro* models, ethanol treatment also obviously reduced the expression level of the endogenous miR-29c and *ADH6* (RNA and protein) levels in Huh7 cells (miR-29c: 27.80% and *ADH6* mRNA: 30.31% in cells exposed to 200 mM alcohol, $P < 0.05$) (Fig. 1d and 1f). Owing to Huh7 cells cultured *in vitro* have little ability to express class I ADH genes or cytochrome P450 2E1. In order to maintain the authenticity of the results, we also tested the miR-29c and ADH6 expression levels in engineered Huh7 cells, which constitutively express the mouse *ADH1* gene ($Huh7^{ADH1}$). As shown in Fig. 1e and 1g, although the miR-29c levels were decreased after ethanol treatment, a slight up-regulation in the mRNA and protein of ADH6 levels occurred after 48 h of exposure to low concentrations of ethanol. When treated with 400 mM ethanol for 48 h, the mRNA and protein levels of ADH6 were decreased dramatically ($P < 0.05$). Taken together, our results indicated that both miR-29c and ADH6 are downregulated by *in vivo* and *in vitro* samples of alcohol exposure.

3.2 Exogenous miR-29c up-regulates ADH6 expression

Based on the results of the above bioinformatics and correlation analysis, we further evaluate whether miR-29c is able to up-regulate ADH6 expression. Different concentrations of miR-29c mimics were transfected into Huh7 and $Huh7^{ADH1}$ cells, respectively. Unlike conventional miRNA functions, as depicted in Fig. 2, together with the elevation of miRNA levels (Fig. 2a), miR-29c significantly increased both mRNA and protein levels of ADH6 in a dose-dependent manner in Huh7 cells (all $P < 0.05$) (Fig. 2b). Similar and more sensitive increases were observed in $Huh7^{ADH1}$ cells (Fig. 2d and 2e). We then wondered whether ectopic miR-29c was able to rescue alcohol-induced ADH6 disorders in cells. As shown in Fig. 2c, upon exposure to a middle-dose (200 mM) of ethanol, the mRNA and protein level of ADH6 were significantly decreased in Huh7 cells, while the addition of low concentration ectopic miR-29c was able to rescue the ethanol-induced ADH6 dysregulation in cells. ADH6, especially the ADH6 protein level, was also significantly rescued by the ectopic miR-29c in a dose-dependent manner in recombinant Huh7cells (Fig. 2f). In summary, our current results show that miR-29c could up-regulate ADH6 expression.

3.3 AGO2 is involved in miR-29c mediated up-regulation of ADH6 expression

Previous studies reported that miRNAs are usually associated with Argonaute (AGO) proteins to direct widespread gene expression at transcriptional or post-transcriptional levels (Gebert & MacRae, 2018). Although there are several AGOs in mammalian cells, AGO1 and AGO2 have positively charged surfaces that are well suited for binding RNA (Janowski et al., 2006). To explore whether the regulatory effect of miR-29c on ADH6 occurs in the presence of AGO1 and/or AGO2 proteins, we performed RNA

immunoprecipitation (RIP) assays using anti-AGO antibodies followed by qRT-PCR using primers specific for miR-29c. Results showed that miR-29c obviously interacted with AGO2, but not AGO1, in which miR-29c levels were 2.89-fold immunoprecipitated by AGO1 antibody, 57.74-fold immunoprecipitated by AGO2 antibody ($P < 0.05$), compared with that of mouse IgG, respectively (Fig. 3A). To further validate the role of AGO1 or AGO2 in the regulatory function of miR-29c on ADH6 expression, siRNAs targeting *AGO1* or *AGO2* genes (Fig. 3b) were co-transfected into Huh7 cells, together with miR-29c mimics or control mimics, respectively. We observed that miR-29c was still able to promote ADH6 expression in AGO1-silencing cells (Fig. 3c). However, in AGO2-silencing cells, the increase of both ADH6 mRNA and protein expression by miR-29c mimics were blocked (Fig. 3d), confirming that AGO2, but not AGO1, participates in the regulatory process of miR-29c on ADH6 expression.

3.4 miR-29c can not bind *ADH6* transcript

We next determined whether there was a direct interaction between miR-29c and *ADH6* transcript. We firstly synthesized biotin-conjugated miR-29c oligonucleotides, and used these oligonucleotides as bait to capture *ADH6* transcript in cells. As shown in Fig. 4a, no significant difference was observed in the pulldown level of *ADH6* mRNA between the miR-29c group and control group, indicating that miR-29c may not bind directly to *ADH6* transcripts in Huh7 cells. To further identify whether miR-29c affects the stability of *ADH6* mRNA, we performed an mRNA stability assay by treating miR-29c transfected or control cells with actinomycin D, a transcription inhibitor. Our data showed that the *ADH6* mRNA stability was almost unaffected in cells transfected with miR-29c mimics (Fig. 4b). In summary, miR-29c cannot bind *ADH6* mRNA and has no effect on the stability of *ADH6* transcript. These data suggest that miR-29c-mediated ADH6 up-regulation is not occurred at the post-transcriptional level.

3.5 miR-29c binds to the enhancer DNA sequence of ADH6 in the presence of cell nuclear extracts

Given that the function of miRNA depends on its cellular location, we subsequently performed nuclear-cytoplasmic fractionation assay, and the qRT-PCR data showed that most endogenous miR-29c is distributed in the cytoplasm (Fig. 5a), which is consistent with previous reports (Liao et al., 2010). However, exogenous miR-29c could move into the nucleus in large quantities after transfection (Fig. 5b), and this result was then verified by cy3-labeled miR-29c mimics transfection while miR-29a was used as the cytoplasmic marker (Fig. 5c). Previous studies have indicated that nuclear miRNAs could interact with various DNA elements, such as enhancers (Xiao et al., 2017), to increase gene transcription. To further assess whether miR-29c interacts with targeted DNA sequence, a part of *ADH6* enhancer, in the nuclear, we synthesized fluorescently labeled short − (19 nt) and long − (43 nt) single-stranded DNA sequences of *ADH6*, which may be the potential binding site of miR-29c based on bioinformatics analysis (Fig. 5d). The results of *in vitro* FREMSA assays showed a distinct mobility shift in lane 7, where the dye-labeled miR-29c and the long DNA oligonucleotides of ADH6 interacted with each other in the presence of nuclear extracts of Huh7 (Fig. 5e). However, there was no binding bands appeared in lane 6, in which only the dye-labeled miR-29c and the long oligonucleotides were added. Furthermore, dye-labeled miR-29c could not bind the short single-strand DNA oligonucleotides and double-stranded DNA oligonucleotides of *ADH6* in

the presence or absence of nuclear extracts (Fig. 5e and Fig S1). Together, those results indicated that miR-29c could bind to the targeted single-strand DNA sequence of *ADH6* enhancer element in the presence of cell nuclear extracts.

3.6 miR-29c activates the target *ADH6* enhancer

To further confirm the activation potential of miR-29c in nuclear, we first investigated whether miR-29c had an effect on the accessible chromatin of the whole nucleus using ATAC-seq. Interestingly, the results showed that the global ATAC-seq signal enrichment increased significantly after transfection of the miR-29c mimics. Next, we analyzed the chromatin accessibility of *ADH6*, which is located on chromosome 4 (chr4:99,200,638 – 99,221,246), based on ATAC-seq. Obviously different enrichment levels of the signal were observed near the enhancer region of *ADH6* (chr4:99,200,638 – 99,221,246, Fig. 6a), which is consistent with our previous bioinformatics results that the binding site of miR-29c to *ADH6* is located in the enhancer region of the ADH6 gene. To investigate the effect of miR-29c on the activity of the targeted enhancer element, we constructed two recombinant pGL3-promoter plasmids in which an ADH6-Wild sequence (containing a 600 nt wildtype flanking sequence) and an ADH6-Mut sequence (containing a 600 nt flanking sequence with mutated enhancer sequence of miR-29c) were inserted (Fig. 6b). Figure 6c showed that exogenous miR-29c transfection significantly increased the luciferase signal produced by the ADH6-Wild reporter in HEK293T, but failed to elevate the luciferase signal produced by the ADH6-Mut reporter as compared with the ones transfected with control mimics. This data indicates that miR-29c can activate its targeted enhancer of *ADH6* gene.

To further study the direct chromatin state alteration of the enhancer, ChIP-qPCR was conducted. As shown in Fig. 6d-6g, compared with non-enhancer regions, although there was no difference in the expression of histones H3, the enhancer region of *ADH6* has more significant H3K27ac and H3K4me1 and H3K4me3 modifications, implying increased chromatin activation in enhancer regions. Together, these results indicated that miR-29c could activate the activity and chromatin state of the targeted enhancer within *ADH6* gene.

3.7 miR-29c up-regulates *ADH* gene cluster in hepatic cells

It is known that enhancer activation is associated with the expression of adjacent genes. ADH genes are distributed in a cluster on chromosome 4 (Fig. 7a). In order to test our hypothesis that miR-29c may also affect ADH gene cluster expression in hepatic cells, we measured the enrichment of RNA polymerase II within the *ADH1A*, *ADH1B*, *ADH1C*, and *ADH4* genes under miR-29c treatment. Results showed that miR-29c significantly elevated the RNA polymerase II enrichment at the promoter regions and exon regions of *ADH1A*, *ADH1B*, *ADH1C*, *ADH4*, and *ADH6* gene (Fig. 7a), indicating transcriptional activation of *ADH* gene cluster. Moreover, miR-29c mimic transfection significantly elevated the pre-mRNA levels of the ADH gene cluster (Fig. 7b-f). Correspondingly, the mRNA expression and protein levels of the *ADH* gene cluster were also increased after miR-29c mimic transfection, although not in a dose-dependent manner (Fig. 7g-7j). Those results proved that miR-29c up-regulates the whole transcriptional levels of *ADH* gene cluster.

4 Discussion

In this study, *in silico* analysis and *in vitro* experiments showed that *ADH6* might be targeted and positively regulated by miR-29c. miR-29c and ADH6 were both significantly down-regulated in ethanol-exposed hepatic cell and ALD patients, and exogenous miR-29c significantly promoted ADH6 expressions without affecting the stability of *ADH6* mRNA. Our following mechanism studies provided multiple prominent findings, including 1) identification that exogenous miR-29c moved into nucleus and bound to the target enhancer DNA sequence; 2) identification that exogenous miR-29c was an enhancer activator; 3) identification that exogenous miR-29c promoted *ADH* gene cluster expression at the transcriptional level.

The miR-29 family, one of the most abundantly expressed miRNAs in human liver, has been reported to be involved in cell differentiation, fibrosis, and apoptosis by regulating its target genes (Horita, Farquharson, & Stephen, 2021; Roderburg et al., 2011). Based on the microRNA microarray, previous studies have reported that has-miR-29c was differentially expressed in alcoholic hepatitis patients compared to normal individuals, but the regulatory mechanism of miR-29c is barely understood. In the present study, we showed that alcohol exposure significantly decreased endogenous miR-29c levels. Bioinformatics analysis that integrates the target prediction, correlation analysis, and free energy analysis identified that miR-29c serves as a positive modulator in ADH6 expression by targeting the coding sequence. We further provided evidence that miR-29c is able to promote the expression of *ADH6* mRNA in both Huh7 and engineered Huh7^{ADH1} cells, providing a new perspective on the mechanism of action of miR-29c in ALD.

Generally, miRNAs are loaded into AGO proteins to form miRNA-containing ribonucleoproteins (miRNPs) to exert regulatory functions. In plants and mammals, there are four AGO clade proteins (AGO1–4), each AGO clade appears to have a different preference for binding small RNAs. For example, AGO1 favors miRNAs with 5'-terminal uridine, while AGO2 primarily binds to small RNAs with 5'-adenosine in *Arabidopsis* (Mi et al., 2008). Our previous reports indicated that the identification of AGO1 is required for the process of miR-148a-mediated ADH4 up-regulation (Luo et al., 2021). However, in the current study, the RIP assay and AGO-knockdown experiment showed that miR-29c directly bound to the AGO2 protein rather than AGO1. Interestingly, AGO2 is the only member of the mammalian AGO protein family that possesses catalytic activity (Papachristou et al., 2011), and plays key roles in regulating gene expression in the nuclei as well as cytoplasm. The nuclear-localized AGO2 gives miRNAs the opportunity to bind intronic and CDS to silence gene expression at transcriptional levels, in addition to 3' UTR (Khan, 2021). In this study, using nucleoplasmic isolation and cy3-labeled mimics transfection, we found that exogenous miR-29c could move into the nucleus in large quantities. Importantly, the exogenous miR-29c cannot increase ADH6 expression in the AGO2-knockdown cells, indicating that exogenous miR-29c promotes ADH6 expression *via* an AGO2-dependent manner in nuclear.

The less studied nuclear miRNAs are now emerging in different physiological and pathological processes. For example, the attenuation of endogenous miR-126-5p nuclear import *via* ablation of Mex3a or ATG5 protein *in vivo* could aggravate endothelial apoptosis and exacerbate atherosclerosis (Santovito

et al., 2020), while the over-expression of exogenous miR-205 readily induced the expression of IL24 and IL32 tumor suppressor genes by targeting specific promoter regions (Majid et al., 2010). Our data showed that exogenous miR-29c could import into the nucleus and bound to its targeted enhancer DNA sequence with the assistance of nuclear proteins. Surprisingly, exogenous miR-29c was able to significantly increase the luciferase activities that produced by the wild type construct (wild ADH6-enhancer construct), but not that produced by the mutant one (ADH6-enhancer Mutation construct), indicating enhancer activation by miR-29c.

In fact, it is not uncommon for non-coding RNAs to act as enhancer activators. The typical example is that an emerging class of regulatory ncRNAs, called enhancer RNAs (eRNAs), are transcribed from enhancers in a tissue-specific manner and in turn directly affect enhancer functions (Li et al., 2013). In addition, many enhancer-like long non-coding RNA (lncRNA) have also emerged here, such as lncRNA NeST (Gomez et al., 2013) and FAL1 (Wu et al., 2019). However, there are few reports of miRNAs being studied as enhancer activators. Only one study reported that miR-24-1 could act as an enhancer trigger to activate neighboring gene transcription by activating enhancer RNA (eRNA) expression, altering histone modification, and increasing the enrichment of p300 and RNA Pol II at the enhancer locus (Xiao et al., 2017). Similarly, we provided evidence in this study that miR-29c is able to activate the chromatin state by increasing H3K27ac and H3K4me1 and H3K4me3 enrichment at the *ADH6* enhancer locus. Furthermore, it is widely accepted that enhancers are a class of cis-acting DNA elements that can activate or enhance gene transcription. Thus, we speculate that the activation of *ADH6* enhancer by miR-29c may further promote the expression of other surrounding genes within the ADH gene cluster. Correlation analysis showed that the expression of miR-29c was positively correlated with *ADH1A*, *ADH1B*, *ADH1C*, *ADH4*, and *ADH6* levels, but had no correlation with *ADH5* and *ADH7* expression. qRT-PCR and immunoblotting data confirmed that exogenous miR-29c significantly enhanced the pre-mRNA, mRNA, and protein levels of ADH1A, ADH1B, ADH1C, ADH4, and ADH6. Meanwhile, we also found that over-expression of exogenous miR-29c altered the global accessibility of chromatin in the cell, which may also be a reason responsible for the up-regulation of the *ADH* gene cluster, which need to be explored further.

Together, we found that miR-29c promotes the expressions of *ADH* gene cluster by targeting and activating the enhancer within *ADH6* gene. In detail, exogenous miR-29c up-regulates ADH6 expressions in an AGO2-dependent manner. miR-29c can import into nucleus and bind the enhancer DNA sequence with the assistance of proteins from nuclear extracts. More importantly, we noted that miR-29c could alter the chromatin status and activate the targeted enhancer, which further increases the expressions of neighboring genes in the *ADH* gene cluster. In summary, our work unravels a novel nonconventional regulatory mechanism of miR-29c for ADH genes. Our findings will provide a theoretical basis for further exploring the roles of miRNA in alcohol metabolism and ALD.

Declarations

Funding

This work was supported by grants from the National Natural Science Foundation of China (81903354, 91943301, and 81973075), and National Key R&D Program of China (2017YFC1600200).

Conflicts of interest

The authors report no declarations of interest.

Ethics approval

Not applicable

Consent to participate

Not applicable

Consent for publication

All authors approved of this submission for publication.

Availability of data and material

All data generated or analysed during this study are included in this published article (and its supplementary information files).

Code availability

Not applicable

Authors' contributions

Jiao Luo and Dianke Yu proposed and organized the study; Jiao Luo and Dianke Yu designed the study; Ningning Chen, Jiao Luo, and Yufei Hou predicted and validated the interaction between miRNA and ADH6. Yanan Ji, Mengyue Xie, and Ge Song performed a visual analysis of the data. Ningning Chen and Jiao Luo wrote the manuscript, and Dianke Yu revised the manuscript. All authors reviewed the manuscript.

References

1. Bajaj, J. S. (2019). Alcohol, liver disease and the gut microbiota. Nat Rev Gastroenterol Hepatol, *16*(4), 235–246. doi:10.1038/s41575-018-0099-1
2. Bala, S., Csak, T., Saha, B., Zatsiorsky, J., Kodys, K., Catalano, D.,.. . Szabo, G. (2016). The pro-inflammatory effects of miR-155 promote liver fibrosis and alcohol-induced steatohepatitis. J Hepatol, *64*(6), 1378–1387. doi:10.1016/j.jhep.2016.01.035

3. Bhatia, S., Drake, D. M., Miller, L., & Wells, P. G. (2019). Oxidative stress and DNA damage in the mechanism of fetal alcohol spectrum disorders. Birth Defects Res, *111*(12), 714–748. doi:10.1002/bdr2.1509
4. Chen, G., Yu, D., Chen, J., Cao, R., Yang, J., Wang, H.,.. . Shi, T. (2015). Re-annotation of presumed noncoding disease/trait-associated genetic variants by integrative analyses. Sci Rep, *5*, 9453. doi:10.1038/srep09453
5. Gao, B., Ahmad, M. F., Nagy, L. E., & Tsukamoto, H. (2019). Inflammatory pathways in alcoholic steatohepatitis. J Hepatol, *70*(2), 249–259. doi:10.1016/j.jhep.2018.10.023
6. Gao, N., Li, J., Li, M. R., Qi, B., Wang, Z., Wang, G. J.,.. . Qiao, H. L. (2018). Higher Activity of Alcohol Dehydrogenase Is Correlated with Hepatic Fibrogenesis. J Pharmacol Exp Ther, *367*(3), 473–482. doi:10.1124/jpet.118.249425
7. Gebert, L. F. R., & MacRae, I. J. (2018). Regulation of microRNA function in animals. Nature Reviews Molecular Cell Biology, *20*(1), 21–37. doi:10.1038/s41580-018-0045-7
8. Gomez, J. A., Wapinski, O. L., Yang, Y. W., Bureau, J. F., Gopinath, S., Monack, D. M.,.. . Kirkegaard, K. (2013). The NeST long ncRNA controls microbial susceptibility and epigenetic activation of the interferon-gamma locus. Cell, *152*(4), 743–754. doi:10.1016/j.cell.2013.01.015
9. Han, S., Yang, Z., Zhang, T., Ma, J., Chandler, K., & Liangpunsakul, S. (2021). Epidemiology of Alcohol-Associated Liver Disease. Clinics in Liver Disease, *25*(3), 483–492. doi:10.1016/j.cld.2021.03.009
10. Haseba, T., & Ohno, Y. (2010). A new view of alcohol metabolism and alcoholism–role of the high-Km Class III alcohol dehydrogenase (ADH3). Int J Environ Res Public Health, *7*(3), 1076–1092. doi:10.3390/ijerph7031076
11. Horita, M., Farquharson, C., & Stephen, L. A. (2021). The role of miR-29 family in disease. J Cell Biochem, *122*(7), 696–715. doi:10.1002/jcb.29896
12. Iwagami, Y., Zou, J., Zhang, H., Cao, K., Ji, C., Kim, M., & Huang, C. K. (2018). Alcohol-mediated miR-34a modulates hepatocyte growth and apoptosis. J Cell Mol Med, *22*(8), 3987–3995. doi:10.1111/jcmm.13681
13. Janowski, B. A., Huffman, K. E., Schwartz, J. C., Ram, R., Nordsell, R., Shames, D. S.,.. . Corey, D. R. (2006). Involvement of AGO1 and AGO2 in mammalian transcriptional silencing. Nat Struct Mol Biol, *13*(9), 787–792. doi:10.1038/nsmb1140
14. Jelski, W., Laniewska-Dunaj, M., Orywal, K., Kochanowicz, J., Rutkowski, R., & Szmitkowski, M. (2017). The diagnostic value of alcohol dehydrogenase (ADH) isoenzymes and aldehyde dehydrogenase (ALDH) measurement in the sera of patients with brain tumor. Arch Med Sci, *13*(2), 346–352. doi:10.5114/aoms.2017.65366
15. Jelski, W., & Szmitkowski, M. (2008). Alcohol dehydrogenase (ADH) and aldehyde dehydrogenase (ALDH) in the cancer diseases. Clin Chim Acta, *395*(1–2), 1–5. doi:10.1016/j.cca.2008.05.001
16. Khan, A. W. (2021). Nuclear functions of microRNAs relevant to the cardiovascular system. Transl Res, *230*, 151–163. doi:10.1016/j.trsl.2020.11.004

17. Li, W., Notani, D., Ma, Q., Tanasa, B., Nunez, E., Chen, A. Y.,.. . Rosenfeld, M. G. (2013). Functional roles of enhancer RNAs for oestrogen-dependent transcriptional activation. Nature, *498*(7455), 516–520. doi:10.1038/nature12210
18. Liao, J. Y., Ma, L. M., Guo, Y. H., Zhang, Y. C., Zhou, H., Shao, P.,.. . Qu, L. H. (2010). Deep sequencing of human nuclear and cytoplasmic small RNAs reveals an unexpectedly complex subcellular distribution of miRNAs and tRNA 3' trailers. PLOS ONE, *5*(5), e10563. doi:10.1371/journal.pone.0010563
19. Liu, Y., Chen, S. H., Jin, X., & Li, Y. M. (2013). Analysis of differentially expressed genes and microRNAs in alcoholic liver disease. Int J Mol Med, *31*(3), 547–554. doi:10.3892/ijmm.2013.1243
20. Luo, J., Hou, Y., Ma, W., Xie, M., Jin, Y., Xu, L.,.. . Yu, D. (2021). A novel mechanism underlying alcohol dehydrogenase expression: hsa-miR-148a-3p promotes ADH4 expression via an AGO1-dependent manner in control and ethanol-exposed hepatic cells. Biochem Pharmacol, *189*, 114458. doi:10.1016/j.bcp.2021.114458
21. Majid, S., Dar, A. A., Saini, S., Yamamura, S., Hirata, H., Tanaka, Y.,.. . Dahiya, R. (2010). MicroRNA-205-directed transcriptional activation of tumor suppressor genes in prostate cancer. Cancer, *116*(24), 5637–5649. doi:10.1002/cncr.25488
22. Marshall, S., Chen, Y., Singh, S., Berrios-Carcamo, P., Heit, C., Apostolopoulos, N.,.. . Vasiliou, V. (2018). Engineered Animal Models Designed for Investigating Ethanol Metabolism, Toxicity and Cancer. Adv Exp Med Biol, *1032*, 203–221. doi:10.1007/978-3-319-98788-0_14
23. Mi, S., Cai, T., Hu, Y., Chen, Y., Hodges, E., Ni, F.,.. . Qi, Y. (2008). Sorting of small RNAs into Arabidopsis argonaute complexes is directed by the 5' terminal nucleotide. Cell, *133*(1), 116–127. doi:10.1016/j.cell.2008.02.034
24. Papachristou, D. J., Korpetinou, A., Giannopoulou, E., Antonacopoulou, A. G., Papadaki, H., Grivas, P.,.. . Kalofonos, H. P. (2011). Expression of the ribonucleases Drosha, Dicer, and Ago2 in colorectal carcinomas. Virchows Arch, *459*(4), 431–440. doi:10.1007/s00428-011-1119-5
25. Rehm, J., Samokhvalov, A. V., & Shield, K. D. (2013). Global burden of alcoholic liver diseases. J Hepatol, *59*(1), 160–168. doi:10.1016/j.jhep.2013.03.007
26. Roderburg, C., Urban, G. W., Bettermann, K., Vucur, M., Zimmermann, H., Schmidt, S.,.. . Luedde, T. (2011). Micro-RNA profiling reveals a role for miR-29 in human and murine liver fibrosis. Hepatology, *53*(1), 209–218. doi:10.1002/hep.23922
27. Rumgay, H., Murphy, N., Ferrari, P., & Soerjomataram, I. (2021). Alcohol and Cancer: Epidemiology and Biological Mechanisms. Nutrients, *13*(9). doi:10.3390/nu13093173
28. Saikia, P., Bellos, D., McMullen, M. R., Pollard, K. A., de la Motte, C., & Nagy, L. E. (2017). MicroRNA 181b-3p and its target importin alpha5 regulate toll-like receptor 4 signaling in Kupffer cells and liver injury in mice in response to ethanol. Hepatology, *66*(2), 602–615. doi:10.1002/hep.29144
29. Santovito, D., Egea, V., Bidzhekov, K., Natarelli, L., Mourão, A., Blanchet, X.,.. . Weber, C. (2020). Noncanonical inhibition of caspase-3 by a nuclear microRNA confers endothelial protection by autophagy in atherosclerosis. Sci Transl Med, *12*(546). doi:10.1126/scitranslmed.aaz2294

30. Satishchandran, A., Ambade, A., Rao, S., Hsueh, Y. C., Iracheta-Vellve, A., Tornai, D.,.. . Szabo, G. (2018). MicroRNA 122, Regulated by GRLH2, Protects Livers of Mice and Patients From Ethanol-Induced Liver Disease. Gastroenterology, *154*(1), 238–252.e237. doi:10.1053/j.gastro.2017.09.022
31. Schmitt, M. J., Margue, C., Behrmann, I., & Kreis, S. (2013). MiRNA-29: a microRNA family with tumor-suppressing and immune-modulating properties. Curr Mol Med, *13*(4), 572–585. doi:10.2174/1566524011313040009
32. Teschke, R. (2018). Alcoholic Liver Disease: Alcohol Metabolism, Cascade of Molecular Mechanisms, Cellular Targets, and Clinical Aspects. Biomedicines, *6*(4). doi:10.3390/biomedicines6040106
33. Thompson, M. G., Navarro, F., Chitsike, L., Ramirez, L., Kovacs, E. J., & Watkins, S. K. (2016). Alcohol exposure differentially effects anti-tumor immunity in females by altering dendritic cell function. Alcohol, *57*, 1–8. doi:10.1016/j.alcohol.2016.10.007
34. Wu, H., Qiao, F., Zhao, Y., Wu, S., Hu, M., Wu, T.,.. . Zhao, J. (2019). Downregulation of Long Non-coding RNA FALEC Inhibits Gastric Cancer Cell Migration and Invasion Through Impairing ECM1 Expression by Exerting Its Enhancer-Like Function. Front Genet, *10*, 255. doi:10.3389/fgene.2019.00255
35. Xiao, M., Li, J., Li, W., Wang, Y., Wu, F., Xi, Y.,.. . Yu, W. (2017). MicroRNAs activate gene transcription epigenetically as an enhancer trigger. RNA Biol, *14*(10), 1326–1334. doi:10.1080/15476286.2015.1112487
36. Yao, J., Cheng, Y., Zhang, D., Fan, J., Zhao, Z., Li, Y.,.. . Guo, Y. (2019). Identification of key genes, MicroRNAs and potentially regulated pathways in alcoholic hepatitis by integrative analysis. Gene, *720*, 144035. doi:10.1016/j.gene.2019.144035
37. You, M., Fischer, M., Deeg, M. A., & Crabb, D. W. (2002). Ethanol induces fatty acid synthesis pathways by activation of sterol regulatory element-binding protein (SREBP). J Biol Chem, *277*(32), 29342–29347. doi:10.1074/jbc.M202411200

Figures

Figure 1

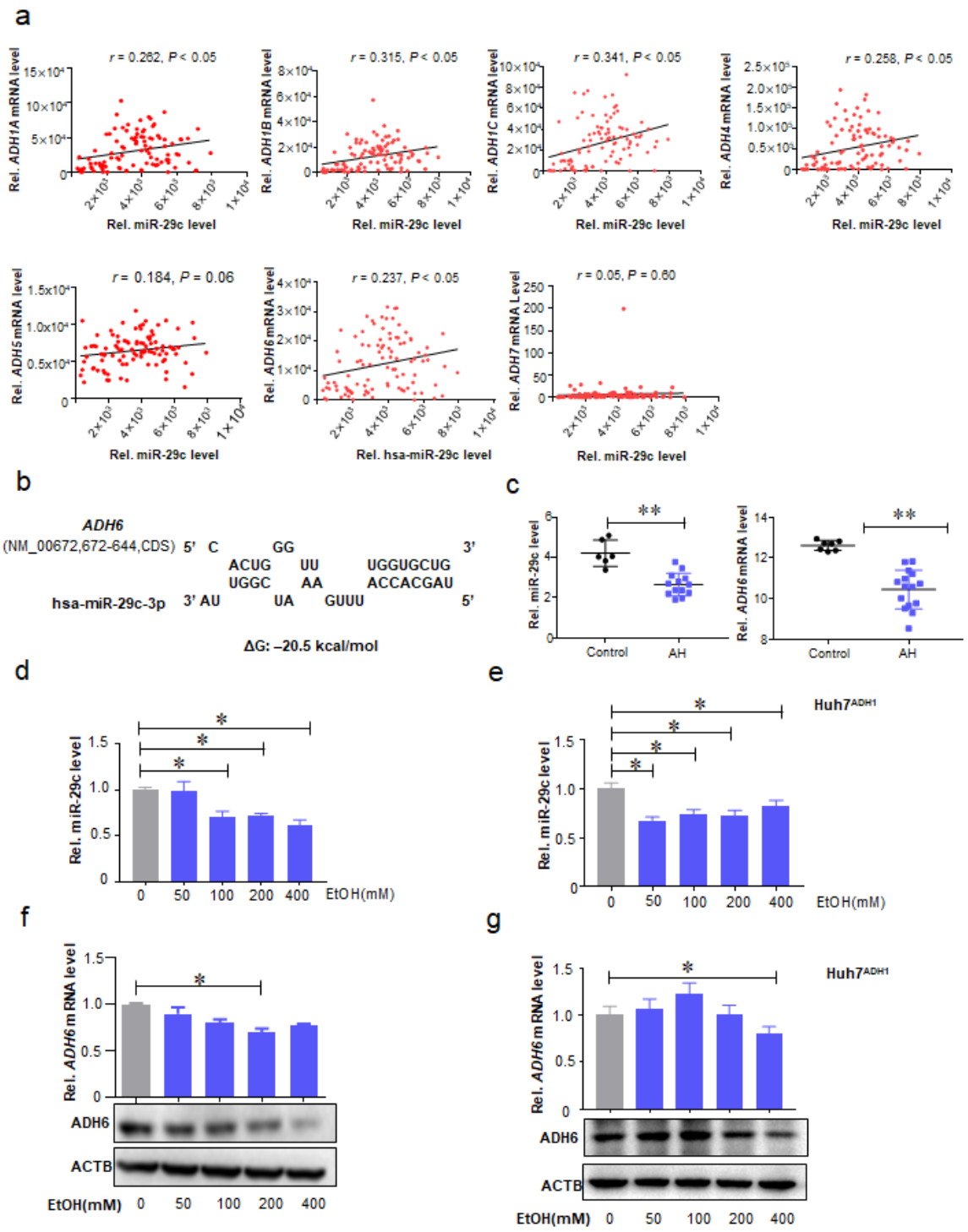

Figure 1

Measurement of endogenous miR-29c and ADH6. (a) The expression correlations between miR-29c and *ADH* genes cluster in human normal liver tissues. The expression profiles were retrieved from TCGA database, and the coefficient (r) was determined by Pearson correlation method. (b) miR-29c were predicted to target *ADH6* by using RNAhybrid tools. (c) Relative expression levels of miR-29c (left) and ADH6 (middle) in the liver samples of patients with alcoholic hepatitis (AH) and healthy controls, and

their correlation analysis (right). Relative miR-29c levels in Huh7 (d) and Huh7^{ADH1} cells (e) after alcohol exposure. Cells were exposed to 0, 50, 100, 200, and 400 mM alcohol for 48 h, respectively, and RNAs were extracted and quantified by qRT-PCR. Relative ADH6 mRNA and protein levels in Huh7 (f) and Huh7^{ADH1} cells (g) after alcohol exposure. Cells were exposed to 0, 50, 100, and 200 mM alcohol for 24 h, respectively. Data are expressed as means ± SD from at least three independent experiments. **P* < 0.05, ***P* < 0.01 and ****P* < 0.001 as indicated, respectively.

Figure 2

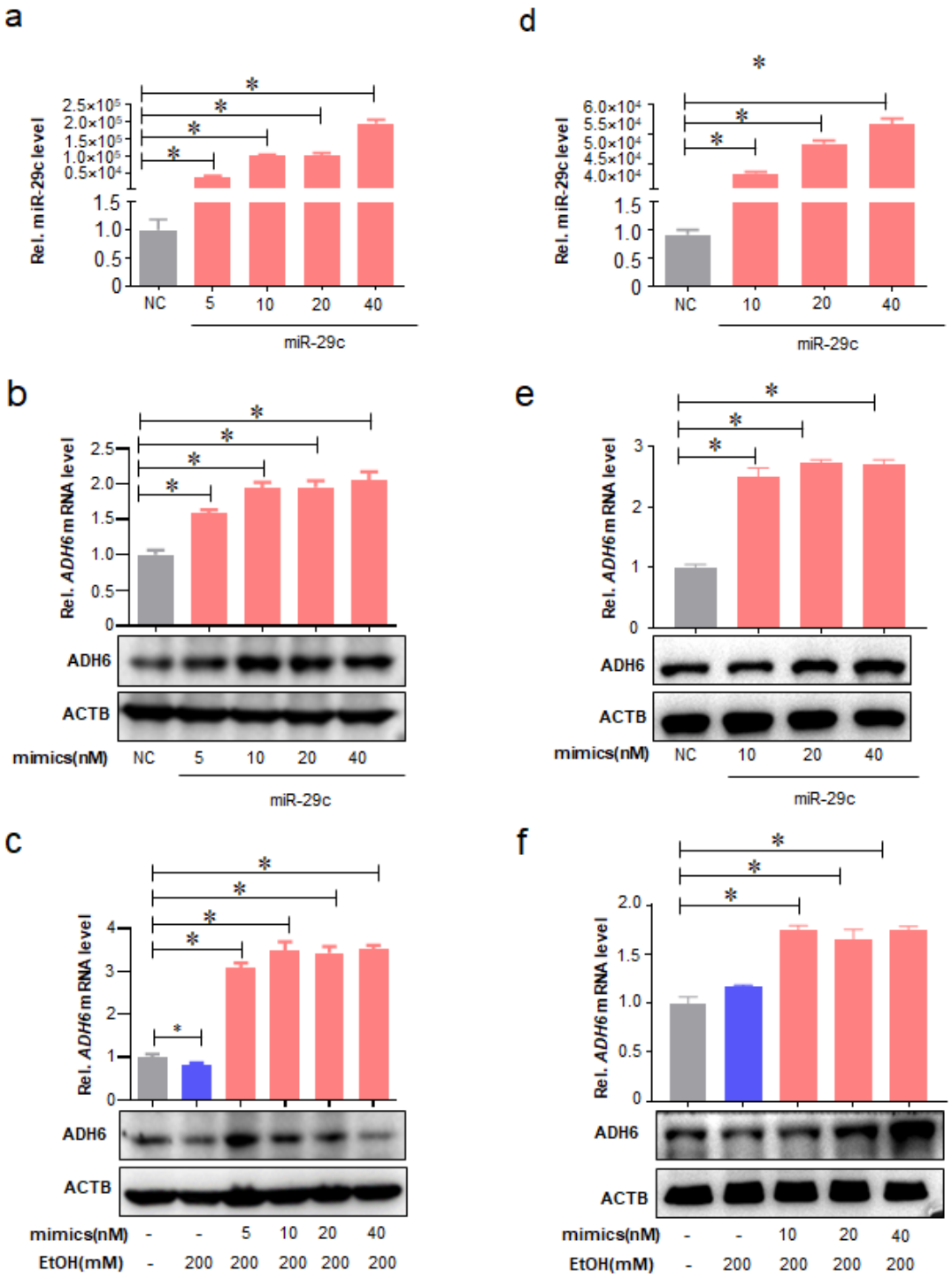

Figure 2

Exogeneous miR-29c regulated the endogenous ADH6 production. Validation of miRNA transfection efficiency in Huh7 (a). Transfection of exogenous miR-29c mimic could significantly up-regulated the endogenous ADH6 expression without (b) or with (c) ethanol co-treatment in Huh7 cells. Similar treatment was also conducted in Huh7^{ADH1} (d-f) cells. After incubation for 24 h, the transfected cells were exposed to 200 mM alcohol for another 48 h. Data are expressed as means ± SD from at least three independent experiments. *P < 0.05, **P < 0.01 and ***P < 0.001 as indicated, respectively.

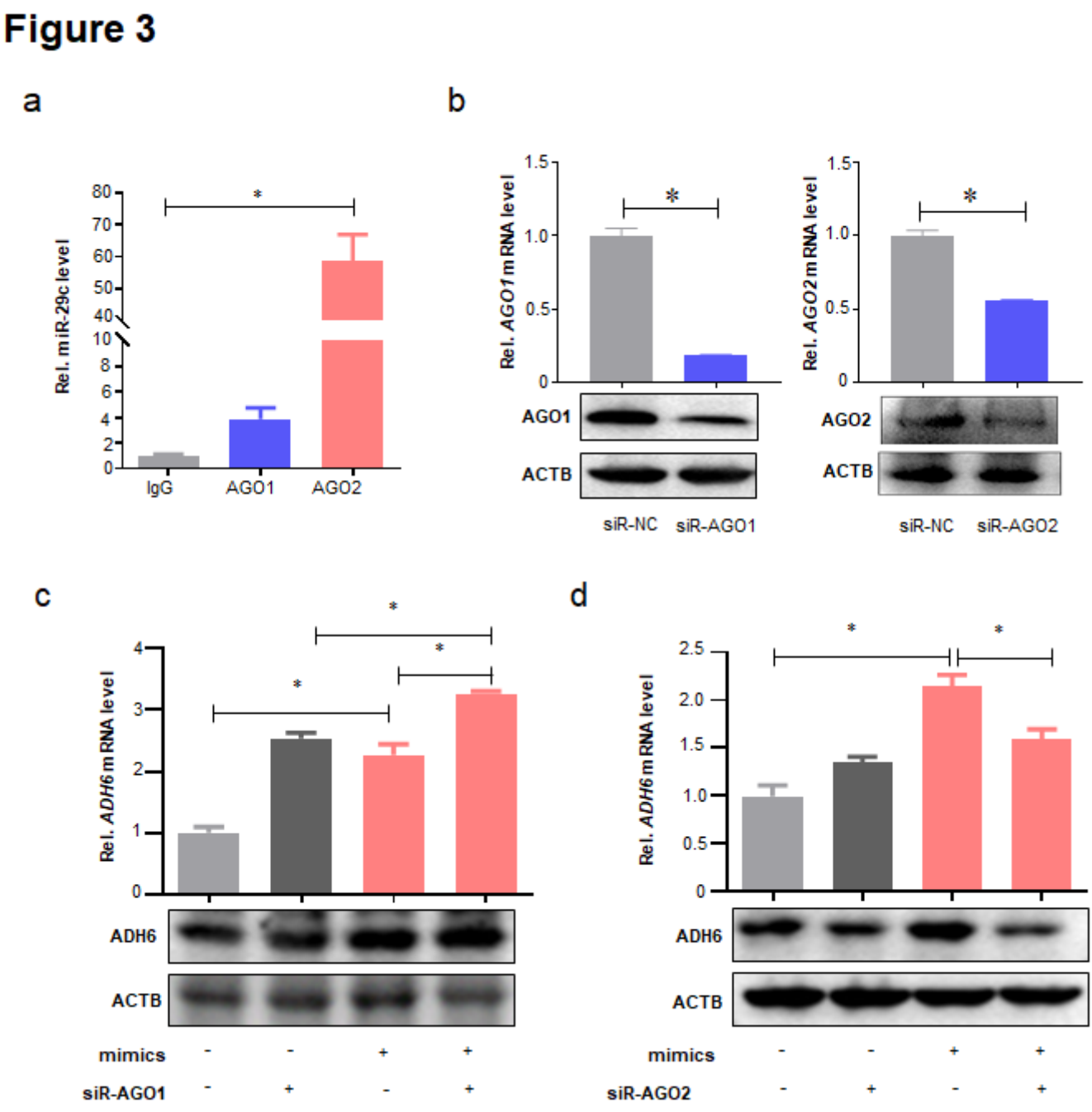

Figure 3

AGO2 is involved in miR-29c-mediated up-regulation of ADH6 expression. (a) RNA immunoprecipitation (RIP) assay was conducted to detect the miR-29c in Huh7 cells, using an antibody against AGO1 and AGO2. The miR-miR-29c enrichment levels were measured by qRT-PCR. (b) Validation of siRNA-AGO1 and siRNA-AGO2 efficiency by qRT-PCR and immunoblotting analysis. (c-d) mRNA and protein levels of ADH6 in Huh7 cells transfected with miR-29c mimics and AGO1 (c) or AGO2 (d) siRNAs. The relative ADH6 mRNA levels were normalized to ACTB in qRT-PCR analysis. Data are expressed as means ± SD from at least three independent experiments. *$P < 0.05$, **$P < 0.01$ and ***$P < 0.001$ as indicated, respectively.

Figure 4

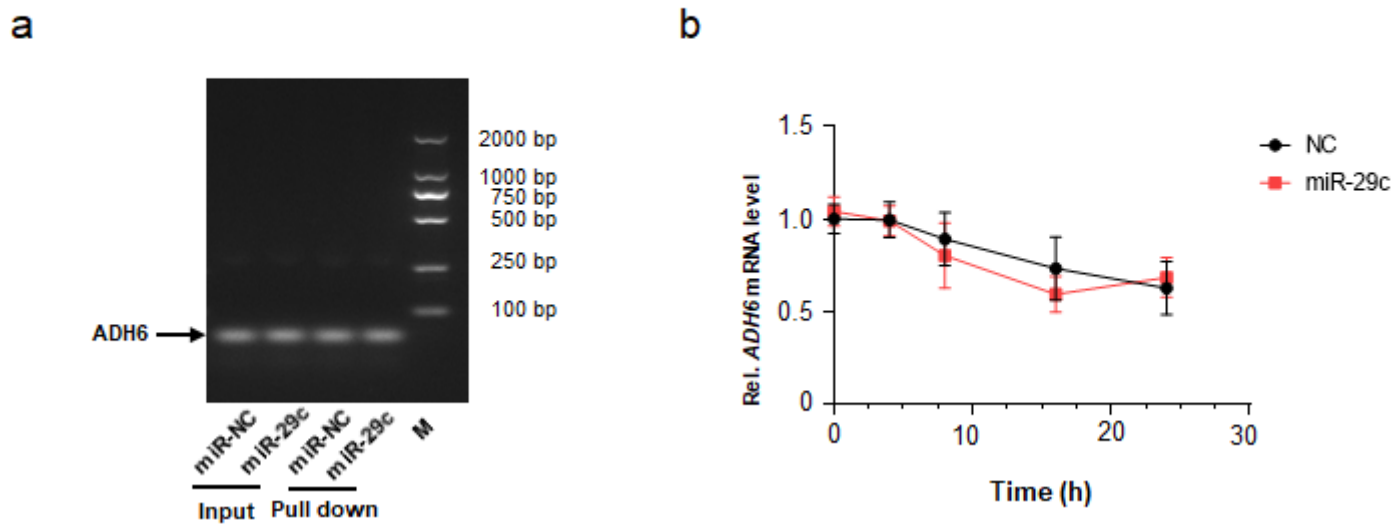

Figure 4

miR-29c does not affect *ADH6* mRNA stability. (a)The ADH6 mRNA was not enriched by streptavidin pull-down for biotinylated miR-29c. (b) The mRNA stability of ADH6 was not affected by miR-29c using actinomycin D treatment. Data are expressed as means ± SD from at least three independent experiments. *$P < 0.05$, **$P < 0.01$ and ***$P < 0.001$ as indicated, respectively.

Figure 5

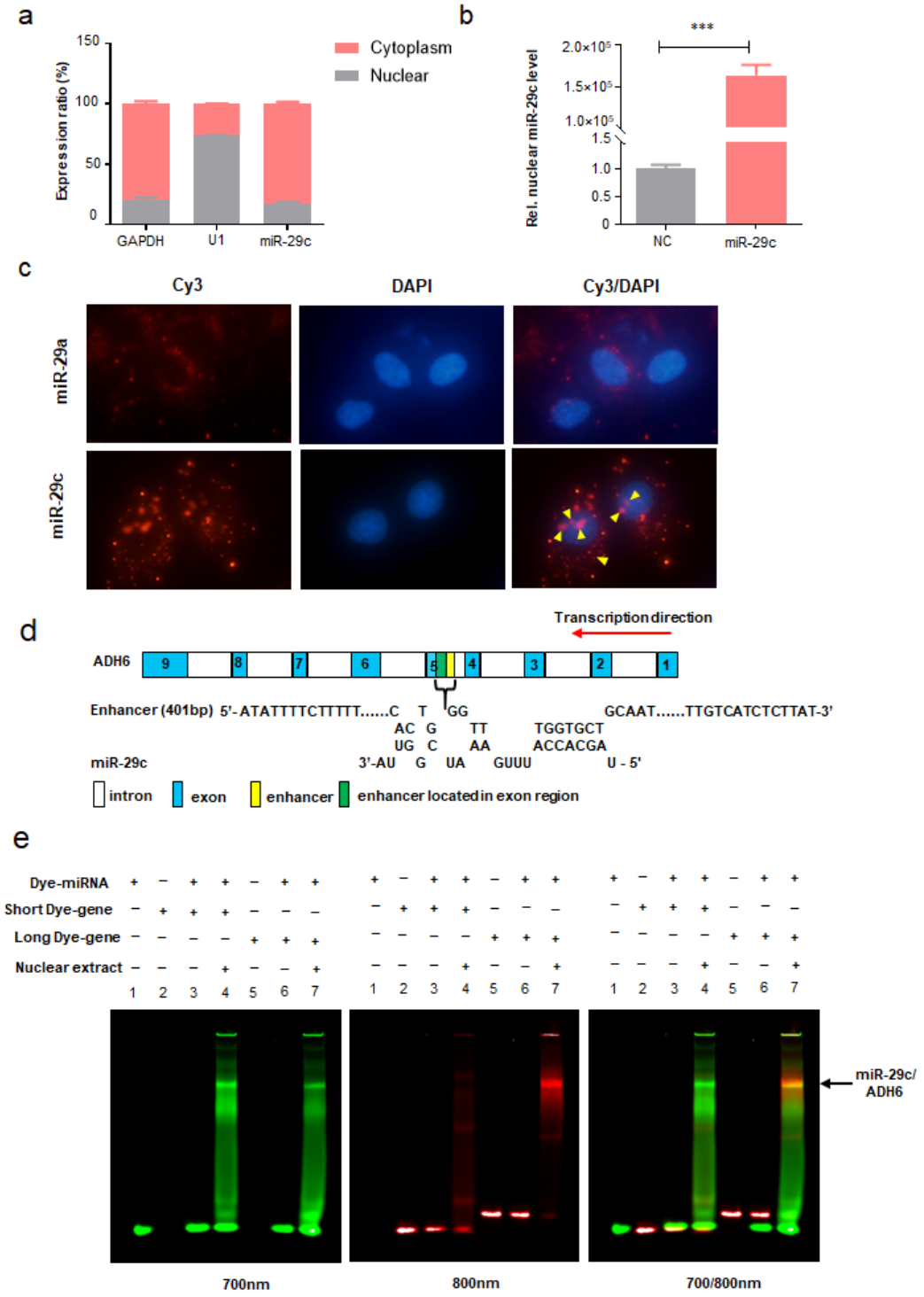

Figure 5

Exogenouse miR-29c binds to the enhancer DNA sequence of ADH6 in the presence of nuclear extracts. (a) miR-29c distribution in the cytosol and nuclei fractions of Huh7 cells. The cytosol and nuclei lysates of Huh7 cells were fractioned, and the miR-29c levels were measured by qRT-PCR. *GAPDH* and *U1* were used as the negative and positive control, respectively. (b) Transfection of miR-29c mimics can enter the nucleus in large quantities compared to the miR-NC. (c) Fluorescence imaging showed that miR-29c

could enter and locate in the nucleus. miR-29a was used as the negative control. (d) The potential miR-29c binding sites within the ADH6 enhancer region. (e) miR-29c binds to the long single-stranded ADH6 DNA sequence and produces a super-shift band. The lanes 1-3 were added with miR-29c probe, ADH6 short-stranded DNA sequence probe, miR-29c probe, and ADH6 short-stranded DNA sequence probe, respectively. The fourth lane adds nucleoproteins on the basis of the third lane. From lanes 5 to 7, change the ADH6 short-chain DNA sequence probe to the ADH6 long-chain DNA sequence probe. Data are expressed as means ± SD from at least three independent experiments. *$P < 0.05$, **$P < 0.01$ and ***$P < 0.001$ as indicated, respectively.

Figure 6

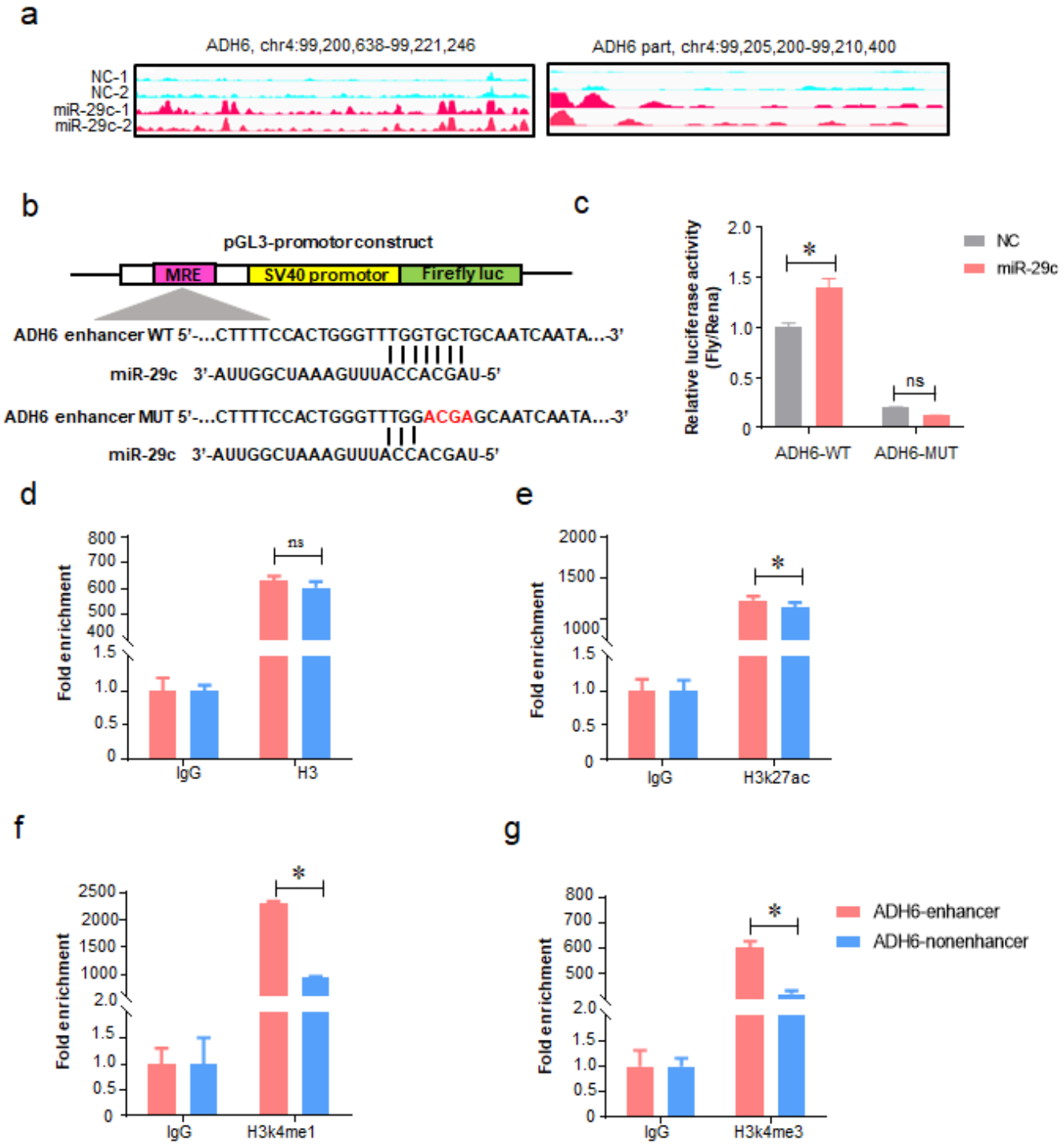

Figure 6

miR-29c activates the enhancer within *ADH6* gene. (a) miR-29c affected the chromatin state of Huh7 cells. Significantly different levels of signal enrichment near ADH6 after transfection of miRNAs compared to controls. (b) The construction of recombinant pGL3-promoter reporter gene plasmid. (c) Relative luciferase activities of ADH6-WT and ADH6-MUT in HEK-293 FT cells. (d-g) ChIP-qPCR analysis

of the chromatin state of the ADH6 enhancer region. Data are expressed as means ± SD from at least three independent experiments. *$P < 0.05$, **$P < 0.01$ and ***$P < 0.001$ as indicated, respectively.

Figure 7

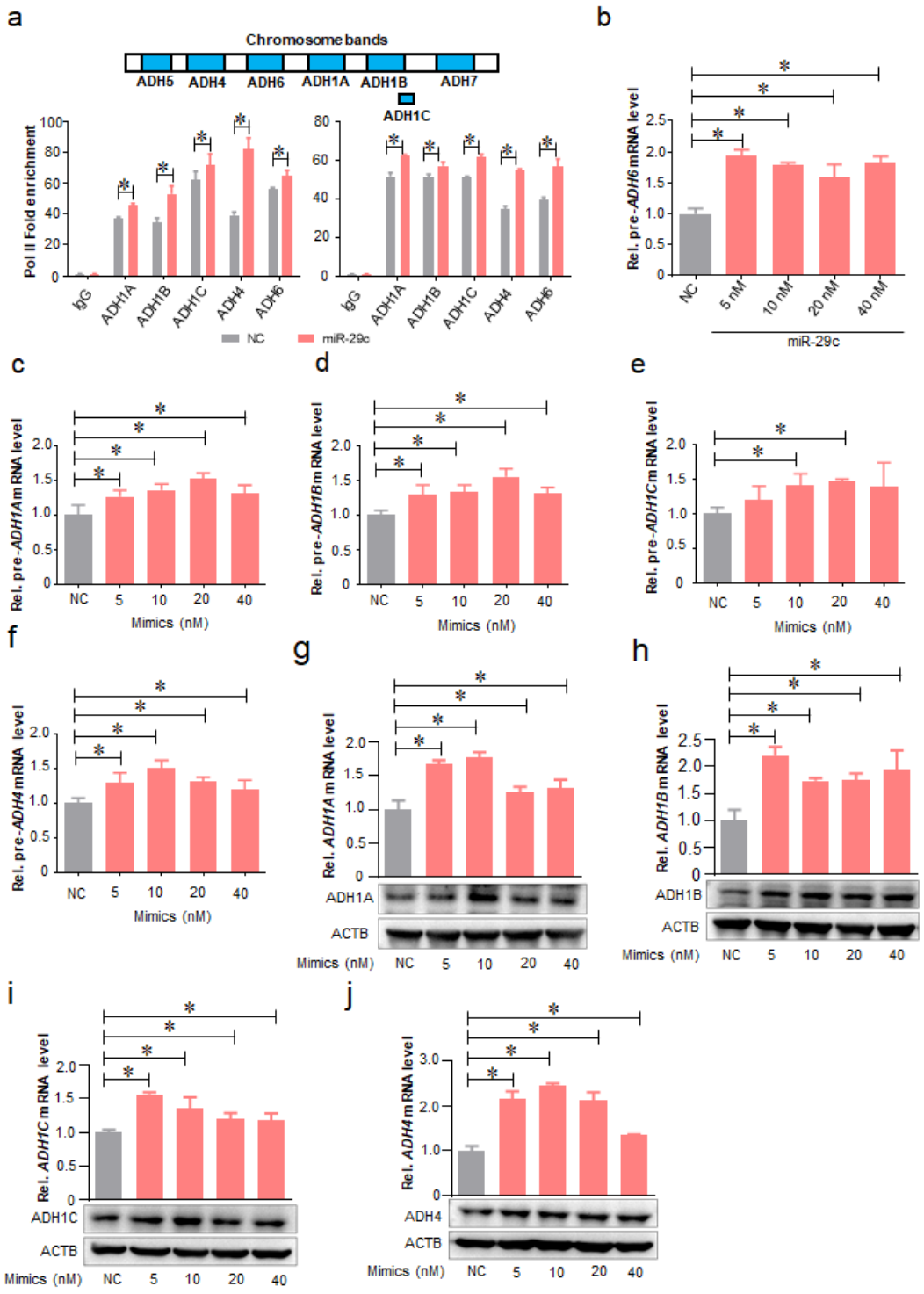

Figure 7

miR-29c promotes the transcription of the ADH gene cluster. (a) Transfection of miR-29c mimics significantly increased the enrichment of RNA polymerase II at the transcription initiation site (left) and

CDS regions of ADH gene cluster (right). (b-f) Transfection of miR-29c mimics significantly induced the pre-mRNA expressions of the ADH gene cluster. (g-j) Relative ADH1A (g), ADH1B (h), ADH1C (i), and ADH4 (j) mRNA and protein levels in Huh7 after miR-29c treatment. Data are expressed as means ± SD from at least three independent experiments. *$P < 0.05$, **$P < 0.01$ and ***$P < 0.001$ as indicated, respectively.

Supplementary Files

This is a list of supplementary files associated with this preprint. Click to download.

- 4Supplementarymaterials.docx
- 1Graphicabstract.pptx